Tailoring the structural, optical, dielectric, and electrical properties of PEO/PVA blend using graphene nanoplates for energy storage devices

Ebtesam M. Alharbi[1] and A. Rajeh[2,*] ⓘ

[1] Department of Physics, College of Science, University of Jeddah, Jeddah, Saudi Arabia
[2] Physics Department, Faculty of Applied Science, Sa'adah University, Sana'a, Yemen

ABSTRACT

Our articles describe the casting process for producing polyvinyl alcohol (PVA)/polyethylene oxide (PEO)/graphene nanoplates (GNPTs) nanocomposites' films. The influence of different concentrations (0.0, 0.05, 0.1, 0.5, and 1%) of GNPTs on the structural, optical, electrical, and dielectric properties of PVA/PEO nanocomposites have been investigated by a Fourier transform infrared (FTIR), X-ray diffraction (XRD), UV\vis spectroscopy, and impedance analyzer. The XRD of the nanocomposite films confirms the enhanced degree of amorphously in the PEO/PVA virgin polymer because of the addition of the GNPTs as nanofiller. The crystallinity decreased from 38.34 to 15.72. The FTIR approves the complexions or interaction of the GNPTs with the polymeric matrix. The optical parameters of the direct and indirect energy gap, as well as Urbach energy, were evaluated using UV/vis absorption spectra in the wavelength range of 200–800 nm. The increase in the concentration of GNPTs resulted in a reduction of the optical band gaps, which reached 1.99 eV for allowed indirect transition. The electric conductivity called AC is the electric conductivity originating potential dependent on frequency. Electrical conductivity is the reciprocal of electrical resistivity, and resistivity can be calculated from resistivity = resistance *Area/Length of a specimen. The composites' ac conductivity varies with frequency according to Jonscher's universal power equation, and it is observed to increase with increasing nanofiller concentrations. At room temperature, the sample containing 1 wt% GNPTs has good optical characteristics, high conductivity, and dielectric constant. The dielectric constants (ε' and ε'') increased as the nanofiller concentration increased and reduced as the frequency increased. Important enhancement in optical, dielectric, and ac electrical properties in these composite films makes them a potential candidate for application in electronic devices.

Address correspondence to E-mail: a.rajeh88@yahoo.com

1 Introduction

Polymer nanocomposites (PNCs) have become a popular study topic in recent years [1–5]. They work in a variety of current industrial and technological applications [6, 7]. This is because they are cheap, have a low density, are flexible, light, and easy to process, can be used in a wide range of industries, and have excellent electrical properties [8]. PNCs with strong optical transparency, high refractive index, and band-gap tenability might also be employed in optoelectronic devices [9]. Two or more miscible polymers are dissolved in a common solvent and blended with a nanofiller of size less than 100 nm to make PNCs, which are made via solution casting. The geometry and size of nanofillers determine their electric, optical, and magnetic characteristics, along with their optoelectronic, electromagnetic, and wave absorption applications [10, 11]. Considering the modest amount of nanofiller used, the electrical, optical, thermal, and structural characteristics of the polymer blends might be significantly improved [12]. There is no covalent bonding in polymer blends which are physical combinations of two or more structurally distinct homopolymers or copolymers that interact by secondary forces. Also, both of these manufacturing polymers dissolve in water, which is a great property for making films [13, 14]. To attain the needed qualities, most companies employ poly (vinyl alcohol) (PVA) as an effective polymer matrix. By doping phosphoric acid with PVA, for instance, a solid polymer electrolyte was created, which may be employed in solid-state electrochromic displays [15]. PVA is a semicrystalline polymer that possesses distinctive physical properties due to crystal-amorphous interfacial phenomena [16, 17]. Owing to the existence of OH groups linking between carbon chain backbone molecules, PVA is one of the biodegradable, nontoxic polymers that enhances electrochemical characteristics [18]. Since the confirmation of the viability of employing PEO as an ion-conductive electrolyte, PEO-based polymer electrolytes have been intensively studied [19]. PEO is frequently employed as a host polymer for producing alkali metal ion-conducting solid polymer electrolytes due to its excellent electrochemical durability, strong solvation, complex formation, and ion dissociation properties [20]. A physical blending of two polymers has been used as an approach for decreasing crystallinity and increasing conductivity in general.

Intermolecular hydrogen bonding between the hydroxyl group of PVA and the C-O asymmetric stretching of PEO is predicted to occur when these two polymers are combined. PVA/PEO mix with high charge storage capacity and dopant-dependent electrical characteristics is also a promising material. Elashmawi et al. studied that the effects of several salts on a PVA/PEO blend have been investigated [21–23]. M. O. Farea et al. studied the effect of cesium bromide on the structural, optical, thermal, and electrical properties of the PVA/PEO blend. They found that the physical properties of polymer matrix were enhanced after the addition of metal halide [24]. Abdelghany et al. suggested that the optical and thermal properties of PEO/PVA were improved by incorporating Ag NPs [25]. The ion electrolytic characteristics of the developed PVA/PEO complexes were favorable for electrochemical applications. To adjust their microstructural features and improve their optical and conductivity properties, these polymer electrolyte systems can be reinforced with nano-sized materials as a next step. In this study, we attempted to develop and implement a novel method of combining two polymeric materials with specific properties that are not available in either of them alone, and then we added some metals in their nanometric form to enhance those properties. We added graphene nanoplates to a PVA/PEO polymeric matrix to enhance its optical and electrical properties for use in a variety of industrial applications. As a result, this research aims to create a PVA/PEO blend-based electrolyte solution complex loaded with nano-sized GNPTs. The various techniques were used to investigate the impact of GNPTs nanoparticles on the microstructural, optical, conductivity, and dielectric characteristics of the resultant PEO/PEO/GNPTs polymer electrolyte nanocomposites.

2 Experimental work

2.1 Chemicals

Solid polymer electrolyte thin films were prepared using the following ingredients in their as-received form. Materials used include polyvinyl alcohol (PVA; molecular weight 14,000 g/mol; purity 99.996%; Sigma-Aldrich), polyethylene oxide (PEO; molecular weight (M.W.) 40,000 g/mol; purity 99.998%;

ACROS, New Jersey, USA), and graphene nanoplates (GNPs); particle size 15 nm; surface area 120–150 m^2/g; Sigma-Aldrich with high purity of 99.999%). For the manufacture of polymeric samples, deionized distilled water was employed as a solvent.

2.2 Synthesis of PVA/PEO–GNPTs nanocomposites

Using distilled water as a solvent, solution-casting films of PVA and PEO (50/50 wt%) blend GNPTs were created. The solution was stirred by a magnetic stirrer at a temperature of 70 °C for 12 h, after which the solutions of GNPTs were immersed in ultrasonic for 1 h and then added to the PVA/PEO solution blend at various concentrations (0.05, 0.1, 0.5, and 1 wt%) with further stirring for 2 h. After that, the solutions were placed into Petri plates and left to gently evaporate at room temperature (RT) for 72 h. The acquired samples, which had a thickness of 0.01–0.2 mm, were peeled from the Petri plates and stored in vacuum desiccators until further measurements (Scheme 1).

2.3 Characterization

Using the Philips X-ray diffractometer XRD system, the X-ray diffraction scans were obtained using CuK$_\alpha$ radiation (where $\lambda = 1.5418$ Å, the tube worked at 30 kV, 2/min speed, the angle of Bragg (2θ) in the 10–80° range). FTIR (Fourier transforms infrared spectroscopy) spectra were taken from 500 cm^{-1} to 4000 cm-1 using a single-beam spectrometer from JASCO, Japan. On a Perkin Elmer Lambda 650 spectrophotometer, the UV–Vis absorption spectra of a
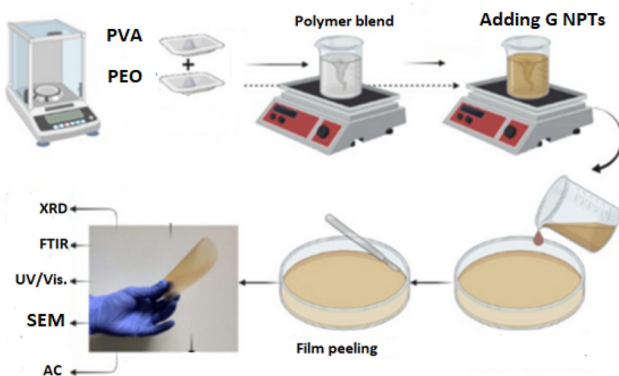
Scheme 1 The preparation process of PVA/PEO-GNPTs' nanocomposites

PVA/PEO blend with various compositions of GNPs nanocomposite were measured in a function range of 200 to 700 nm. Scanning electron micrograph of the prepared samples was achieved using SEM Model (JEOL JSM 6510 LV 250, USA), operating at 20 kV accelerating voltage. To minimize sample charging effects due to the electron beam, the surface of the samples was coated with a 3.5 nm layer of gold. A Novocontrol turnkey 40 system high-performance frequency analyzer measured the conductivity and dielectric constants at frequencies between 0.1 Hz and 20 MHz, accounting for the effects of temperature.

3 Results and discussions

3.1 XRD

Figure 1a, b presents X-ray diffraction patterns of the GNPTs nanopowder and pure PVA/PEO and PVA/PEO/GNPTs nanocomposites films. The semicrystalline structure of this host polymer mix matrices was confirmed by the presence of two significant intense and sharp peaks in the pure PVA/PEO blend film, which we ascribe to the PEO reflection planes (i.e., 19.19° (120) and 23.35° (112), (032)) [23, 26]. The relative shifts in the XRD patterns of the PVA/PEO mix, caused by the incorporation of GNPTs, demonstrate that the host matrix of these polymer nanocomposites has undergone a substantial modification. First, it was shown that the PEO peaks' intensities are much lower, showing a substantial reduction in the crystalline quantity of the host matrix. Second, increasing the nanofiller quantity from 0.1 to 1 wt% resulted in a progressive rise in the intensity of the GNPTs peaks, indicating the existence of filled GNPTs inside the host PVA/PEO combination matrix. There was primarily electrostatic contact between the blended chain structures of the PVA and PEO and the loaded GNPTs, as evidenced by the fact that the location of the GNPTs peak in the host matrix fairly coincided with that of its pristine nanopowder peaks. From the viewpoint of nanocomposite creation, these structural data show that the generated polymer nanocomposites are of high quality. Using the relation based on the integrated area of polymer diffraction peaks and the hump area in the XRD traces across the range 5° to 40°, the values of percent crystallinity Xc (%) of the PVA/PEO blend and
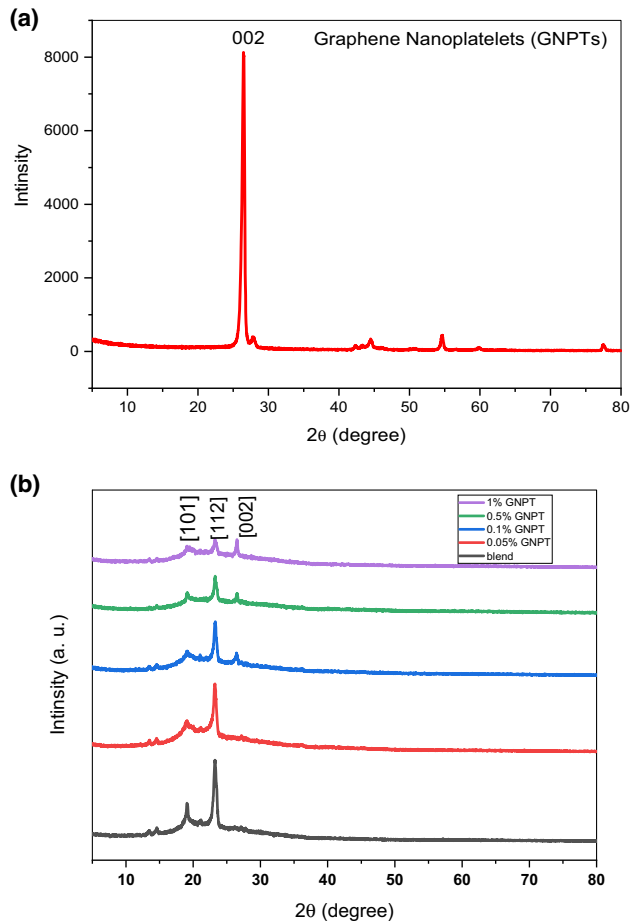
Fig. 1 XRD patterns of **a** pure graphene nanoplate, and **b** pure PVA/PEO doped with various contents of the GNPTs

polymer nanocomposites films were determined (as given in Table2) [27]. From Table 2, we observed the values of percent crystallinity Xc (%) decreased as a result of doping, which indicates the decrease of crystallinity (are getting more amorphous) in the PNCs films. A plausible explanation for this phenomenon is that the polymer chains interact with the GNPTs fillers, resulting in a reduction of the intermolecular connection between the polymer chains [28]. This improves the suitability of using the polymer film as an electrolyte in energy storage devices by allowing polymer chains to move freely within the amorphous domain, which in turn promotes the mobility enhancement of the charge carriers in the polymer electrolytes and leads to an increase in ionic conductivity [29, 30].

3.2 FTIR

To understand how the graphene nanoplates and polymers in the nanocomposites interact with each other, an FTIR analysis is performed. Figure 2a displays the spectral characteristics that differentiate pure PVA/PEO films from PVA/PEO/GNPTs nanocomposites films. Table 1 shows the wave numbers that correspond to significant peaks and their assignments for these films. For the PVA/PEO polymer blend of graphene nanoplates, the simultaneous presence of (OH, C = O) in PVA and (C–O–C) in PEO suggests that the blend sections are miscible. PEO is particularly well suited to forming
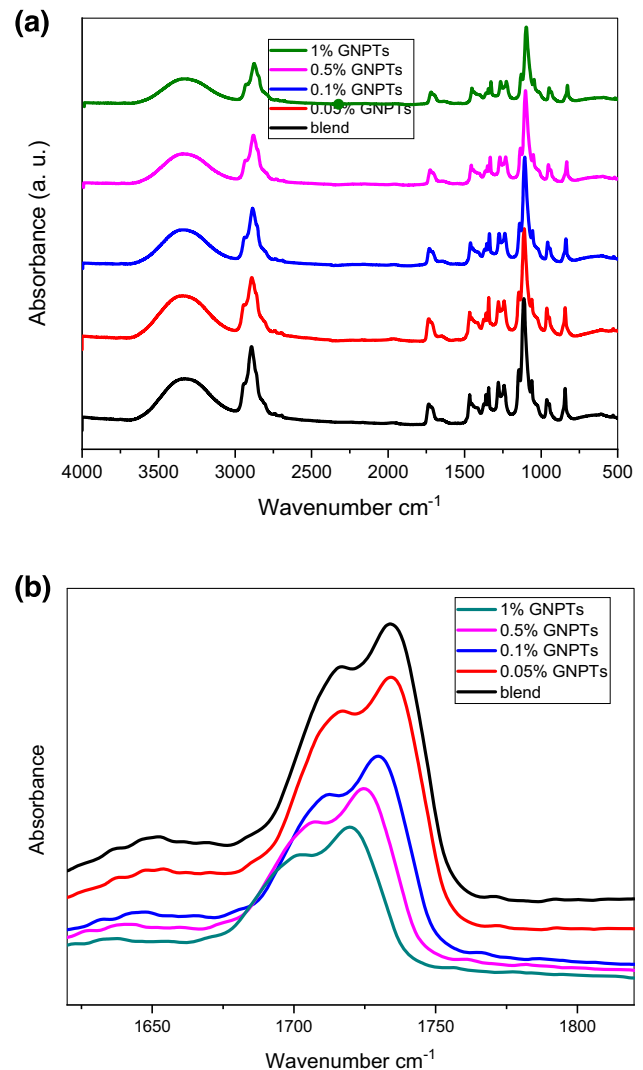

Fig. 2 FTIR spectra of pure PVA/PEO doped with various contents of the GNPTs films **a** 4000–500 cm^{-1} and **b** 1670–1850 cm.$^{-1}$

Table 1 The FTIR of the vibrational assignment for the prepared films

Assignment	Wavenumber (cm^{-1})
O–H stretching	3330
CH asymmetric stretching of CH$_2$	2940
C=O stretching	1735
C–C stretching	1427
Symmetric & asymmetric C–O–C stretching	1095
C-O stretch	1065

intermolecular hydrogen bonds with a wide range of substances that are very electronegative. Electronegative oxygen and hydroxyl groups found in PVA polymer are presumably treated as exceptional proton acceptors [31]. Pure blend FTIR spectra show high bandwidth at 3330 cm^{-1}, demonstrating the mix's O–H stretching vibrations. Absorption peaks in pure PVA/PEO blend can be seen at 2940 cm^{-1}, which are associated with -CH$_2$ asymmetric stretching and -CH asymmetric stretching, 1735 cm^{-1}, which is associated with amide C = O stretching, 1427 cm^{-1}, which is associated with C–C stretching and -CH$_3$ bending, and 1065 cm^{-1}, which is associated with C–O stretching and vibration [32]. The existence of GNPTs in PEO/PVA-GNPTs nanocomposites slightly changes the position (at 1735 cm^{-1}) and intensity of the peaks as shown in Fig. 2b. These results suggest that the PVA/PEO matrix and the GNPTs interact strongly (see Scheme 2).

3.3 SEM analysis

The SEM technique was used to analyze the polymer films' surface morphology. SEM images of pure PVA/PEO and nanocomposites films are shown in Fig 3. The dark background is the pure PVA/PEO film. Figure 3 (0.05%, 0.5%) makes it clear that white clusters of various sizes developed on the sample surface. It is important to note that the white aggregated GNPTs nanoparticles in the PVA/PEO matrix are visible in the image film in Fig. 3 (1%) and uniformly distributed on the surface of the film. A homogeneous surface with a less porous structure and a uniform dispersion of nanoparticles are seen through SEM examination [32]. This suggests PEO and PVA good compatibility. All the prepared polymer nanocomposites' surfaces are smooth without noticeable defects. Moreover, the particle size increases which is in good accordance with the XRD result. Also, SEM images showed that the PVA/PEO-GNPTs films have no air bubbles.
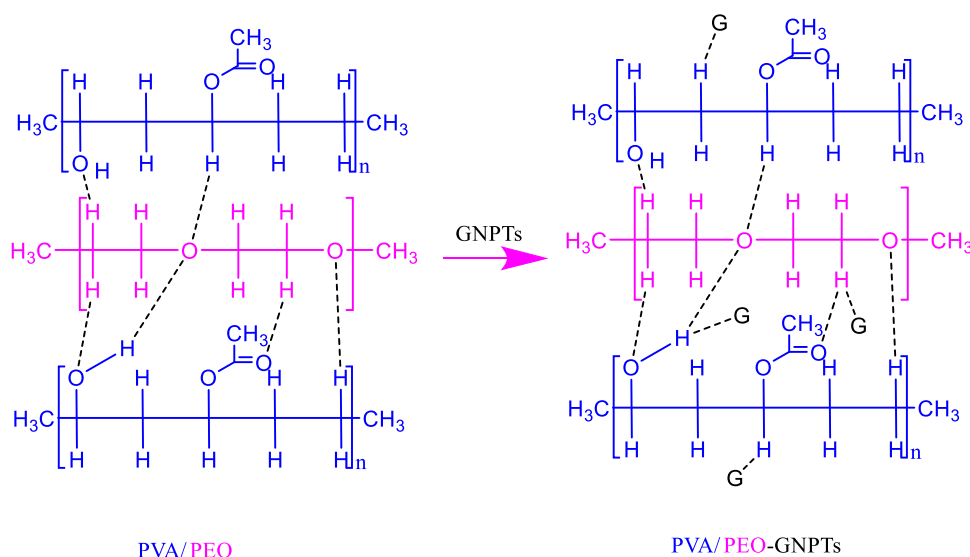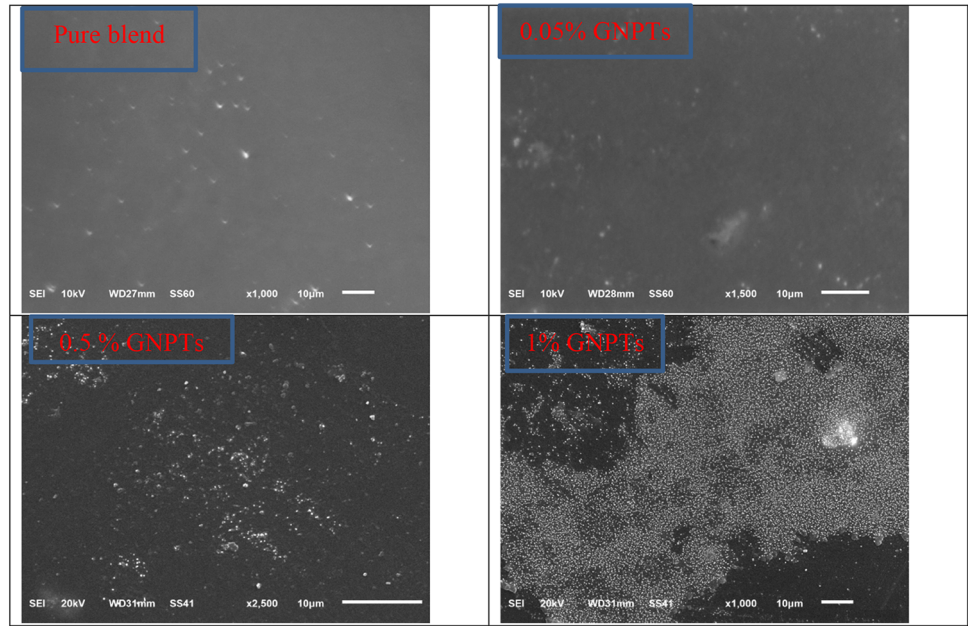
Scheme 2 The potential mechanism for interaction between PVA/PEO blend and GNPTs

PVA/PEO   PVA/PEO-GNPTs

Fig. 3 SEM images of pure PVA/PEO doped with various contents (0.05, 0.5, and 1 wt%) of the GNPTs' films

3.4 Optical property analysis

Figure 4 displays the wavelength-dependent absorption spectra of pure PVA/PEO and modified PVA/PEO containing various concentrations of GNPTs. The strength of absorption in the spectrum of each sample reduced as wavelength rose, whereas it increased as GNPTs amounts increased. At high wavelengths, the films are seen to be nearly transparent. The spectra of pure composite showed an absorption edge at roughly 210 nm, and with each sample, an obvious shift of the absorption edge to a longer wavelength was seen. It was hypothesized that the presence of the π—π* electronic transition, typical of the conjugated (C = O) group, accounted for the 200–300 nm absorption band seen in all of the samples [33, 34].

As demonstrated in Fig. 3, the optical absorbance spectrum may be utilized to compute the absorption coefficient (α) as in Fig. 5.

$$\alpha = \frac{(2.303)A}{d}, \qquad (1)$$

where d signifies the thickness of the film and A is the absorbance. The absorption coefficient was increased with increasing graphene nanoplates concentrations.

Tauc's equation was used to calculate the energy gap of PVA/PEO samples doped with GNPTs [35]:
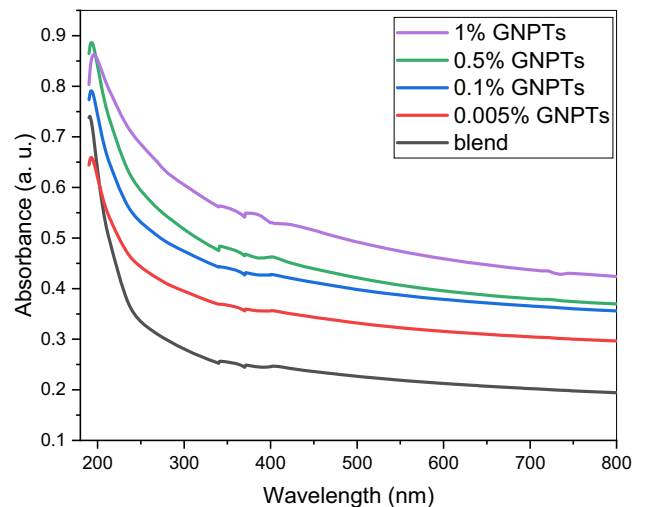

Fig. 4 UV–Vis absorption spectra for the pure PVA/PEO doped with various contents of the GNPTs films

$$\alpha h\upsilon = B\left(h\upsilon - E_g\right)^n. \qquad (2)$$

Hence, n is the variable factor between the direct transition ($n = 1/2$) and the indirect transition ($n = 2$), B is a constant, Eg is the band-gap energy, and α is the absorption coefficient. The direct and indirect band gaps are two of the most essential characteristics that may be determined using Tauc's equation. Figure 5a, b demonstrates the relationship between $(\alpha h\upsilon)^2$ and $(\alpha h\upsilon)^{1/2}$ as a function of photon energy (hυ). Table 2 is a summary of the values for the direct (E_{gd}) and
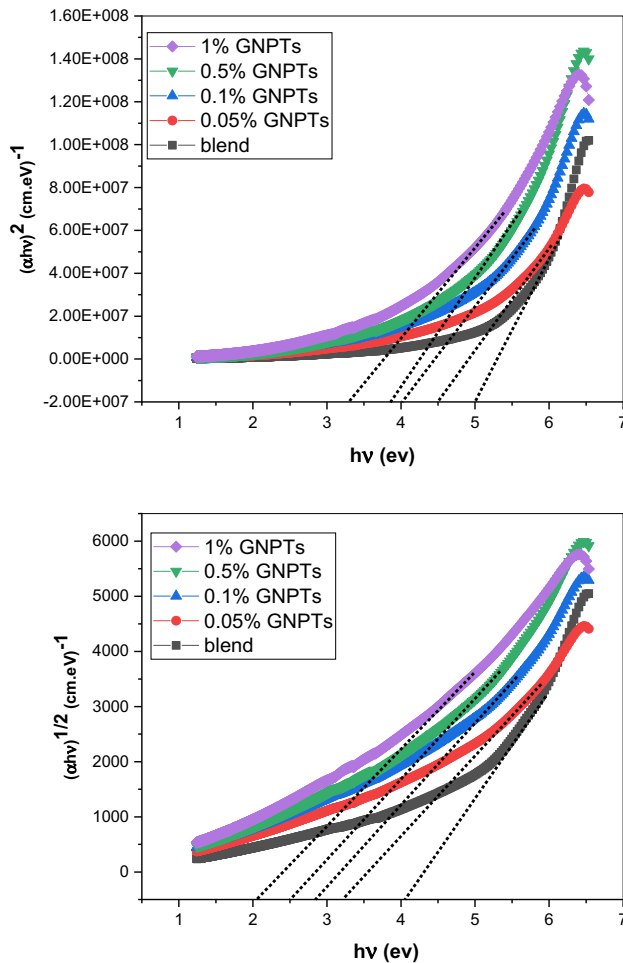
Fig. 5 Plots of (**a**) $(\alpha h\upsilon)^2$ and (**b**) $(\alpha h\upsilon)^{0.5}$ ($h\upsilon$) for pure PVA/PEO doped with various contents of the GNPTs films

indirect (E_{gi}) band gaps that were calculated from the figure. Redshifts in E_{gd} and E_{gi} values from 5.02 eV to 3.25 eV and from 4.06 eV to 1.99 eV, respectively, are easily observed when GNPT concentrations in the matrix increase to 1 wt.%. This is consistent with XRD findings that show a reduction in polymer crystallinity following the incorporation of GNPTs [36, 37]. Moreover, this is due to the impurity introduced into the matrix, which resulted in the formation of inter-band levels and, therefore, led to disordering in the

fabricated composites [38]. So, the gap between the bands also decreases slightly. By calculating the Urbach energy (E_U) with the assistance of the empirical relation of the absorption coefficient, we can demonstrate that the disordering degree of the polymer samples has increased [39]:

$$\alpha(\upsilon) = \alpha_\circ e^{(h\upsilon/EU)}, \tag{3}$$

where α_0 represents a constant and E_U stands for the Urbach energy. For the area close to the absorption edge, the relation between $Ln(\alpha)$ and photon energy ($h\upsilon$) is depicted in Fig. 6. The result is a linear relationship that obeys Eq. (3). As shown in Table 2, the values of the E_U may be calculated using the inverse slope. As the concentration of GNPTs in the PVA/PEO matrix rises, the E_U value rises as well. This indicates that the disordering degree of the polymer sample structure has increased, as has the number of localized states in the prohibited band gaps [40, 41]. The XRD results confirm this speech, as we noticed that the peaks at 19.19 and 23.35 increased in broadness with increasing the concentrations of the graphene nanoplates. Also, Table 2 shows a decrease in the degree of crystallization with the increase in the concentration of the graphene nanoplates, which means the disordering degree of the polymer sample structure has increased. Another evidence, the electrical conductivity of the prepared samples has been increased, which means the disordering degree of the polymer sample structure has increased. In addition, the probability of transitions rises as one moves from the band to the tail, as well as from the tail to the next tail. Urbach energy is a measure of the average of the energies of photons, strong ionic bonds, and thermal vibrations; it is also connected to static and induced disorders [42].

3.5 Electrical measurements

3.5.1 AC conductivity

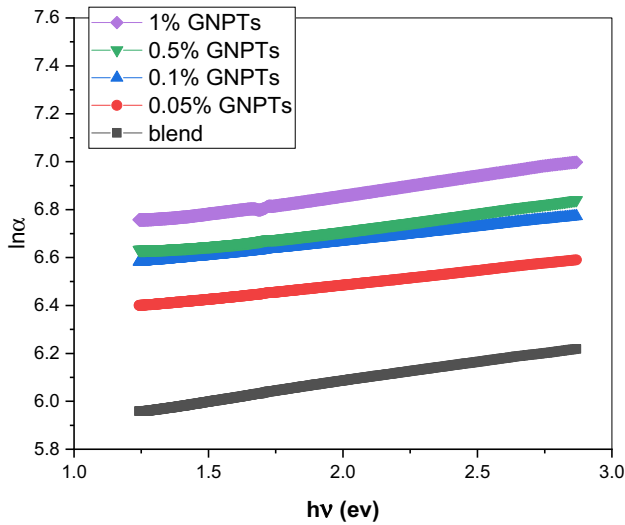Figure 7 depicts the frequency-dependent AC conductivity spectra of PVA/PEO and PVA/PEO/

Table 2 Values of Eg, Eu, relaxation time (s), and Xc for pure PVA/PEO doped with various contents of the GNPTs films

Samples	$E_{g\ direct}$	$E_{g\ indirect}$	Eu	Relaxation times (s) at RT	Xc
Pure blend	5.02	4.06	0.19056 ± 0.0011	6.23×10^{-2}	38.34
Blend/0.05% GNPTs	4.55	3.23	0.2314 ± 0.00104	5.65×10^{-2}	33.54
Blend/0.1% GNPTs	4.05	2.90	0.2557 ± 0.00109	9.23×10^{-3}	25.98
Blend/0.5% GNPTs	3.68	2.55	0.2886 ± 0.00108	3.78×10^{-4}	20.34
Blend/1% GNPTs	3.25	1.99	0.3145 ± 0.00103	9.78×10^{-4}	15.72

Fig. 6 The relation between Ln(α) vs. (hυ) for pure PVA/PEO doped with various contents of the GNPTs films
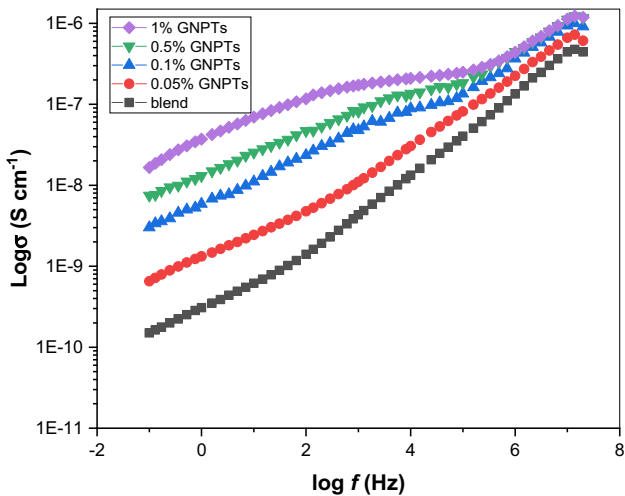

Fig. 7 Ac conductivity of pure PVA/PEO doped with various contents of the GNPTs films at room temperature

GNPTs nanocomposites films at RT. In Fig. 7, we can see three unique zones in the frequency-dependent conductivity plots: the low-frequency dispersion zone, the frequency-independent plateau zone, and the high-frequency dispersion zone. Electrode–electrolyte or space-charge polarization mechanisms cause low-frequency dispersion [42]. The electrode–electrolyte contact accumulates a greater charge in the low-frequency zone. It has been found that the conductivity of PVA/PEO electrolytes is related to the presence of a frequency-independent plateau zone. The long-range migration of the nanofiller ion is responsible for the conductivity that appears in the plateau area. Charge-carrier accumulation causes a third area in which conductivity increases at higher frequencies relative to intermediate frequencies in pure and nanocomposites films. As demonstrated in Fig. 7, the ac conductivity rises as the nanofiller concentration rises, owing to an increase in the number of mobile charge carriers caused by the incorporation of GNPTs [43]. As a result, the mobility of anions has been reduced, while the mobility of GNPTs' cations has increased the conductivity of the polymer composite. In addition, it is observed that the ac conductivity of GNPTs-doped PVA/PEO samples is greater than that of pure PVA/PEO blend. For GNPTs (1 wt%) doped PVA/PEO film, the highest conductivity was found to be 6.89 9 10^{-7} S/cm at 5 MHz. Furthermore, it seems from the graph that the conductivity significantly rises with increasing frequency. At high frequencies, the bonds begin to spin, resulting in a dielectric transition with an accessible, flexible polar bond. Chemical modifications in the polymeric chains will result from the production of complicated charge transfer, which will improve dielectric and AC conductivity [5, 44].

3.5.2 Dielectric analysis

The amount of energy stored in a material is quantified by its dielectric constant. For pure PVA/PEO and PVA/PEO-GNPTs nanocomposites samples, Fig. 8 depicts the plot of (a) real part ε' and (b) imaginary part ε'' of dielectric constant as a function of frequency. The dielectric constant is shown to be maximum at low frequencies and to reduce with increasing frequency. The Maxwell Wagner two-layer model, which is usually applicable to heterogeneous systems, may explain the high values of dielectric constant in the low-frequency region caused by the interfacial space-charge polarization [45]. It demonstrates that the low-frequency dispersions are quite significant and may be attributed to space-charge polarization effects caused by the electrodes. Because of the strong periodic reversal of the field at the interface, the contribution of charge carriers to the dielectric constant reduces with increasing frequency in the higher-frequency zone. As a result, as frequency increases, the dielectric constant reduces [46]. The dielectric constant of the PVA/PEO film is found to rise when the concentration of GNPTs is raised, confirming that their inclusion raises the film's dielectric properties.
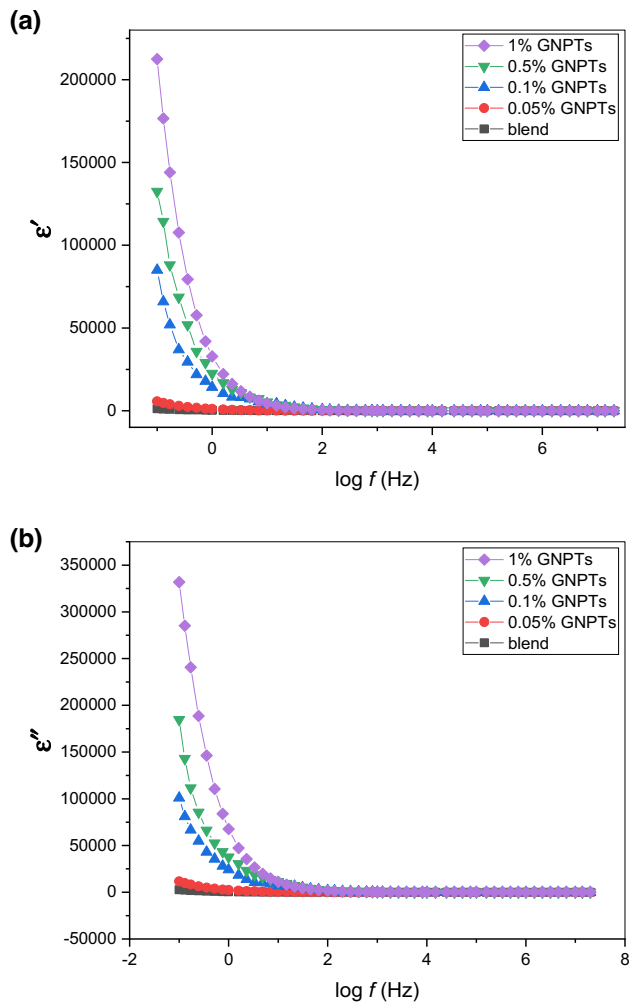
(a)

(b)

Fig. 8 Dielectric plots **a** ε′ and **b** ε″ of pure PVA/PEO doped with various contents of the GNPTs films at room temperature

4 Conclusion

The optical and electrical characteristics of PVA/PEO nanocomposites samples incorporated with various concentrations of GNPTs (0.0%, 0.05%, 0.1%, 0.5, and 1%) were investigated in this study. The creation of a charge-transfer complex between the GNPTs and the PVA/PEO is shown by the shift and reduction in the intensity of the FTIR spectra of the blend filled with 1 wt% of GNPTs. The incorporation of GNPTs enhanced the amorphous domains of the polymer composite, according to XRD measurements. The addition of extra energy levels between the valence band and conduction band is responsible for the reduction in the energy gap from 5.02 eV for pure PVA/PEO to 3.25 eV for PVA/PEO filled with 1 wt. Electrical conductivity measurements revealed that

when the amount of GNPTs and frequency rise, so does the conductivity. To understand how dipoles or charges get polarized, scientists have turned to Maxwell's and Wagner's two-layer models, which predict a reduction in dielectric constant and dielectric loss with frequency as seen in our research. Changes in alternating conductivity are supported by variations in the dielectric properties. The main function of GNPTs is to increase the charge carriers inside the polymeric chains (PVA/PEO) because this material is characterized by its huge specific surface area, a large percentage of surface atoms, and the insulating behavior, so GNPTs an electrostatic material with remarkable cubic and electrochemical spinel structure features, making it excellent as an energy storage material. Increasing the dielectric constant (ε′) means increasing the storage capacity of the material, which makes it more suitable for future materials used in memory devices such as NANDs, DRAM, solar cells, and so on. The current polymer nanocomposites satisfied the requisite optical and electrical characteristics, indicating that they might be employed in electronic applications such as separators in batteries, storage devices, and thermoelectric devices, all of which need further analysis.

5 Recommendations

1 The best way to take advantage of some of these new physical characteristics is the incorporation of nanoscopic metal structures into polymeric matrices.
2 Polymer-embedded nanostructures are potentially useful for a range of technical applications in particular as advanced functional materials (e.g., high-energy radiation shielding materials, microwave absorbers, optical limiters, polarizers, sensors, hydrogen storage systems, etc.).

Author contributions

EMA Investigation, Conceptualization, Writing – review & editing. AR Methodology, Formal analysis, Investigation, Original draft, Writing – review & editing.

Funding

Data availability

The authors confirm that the data supporting the findings of this study are available within the article.

Declarations

Conflict of interest The authors declare that they have no conflict of interest.

Ethical approval The authors have found all the moral standards and will intended to follow them in the future.

References

1. A.S. Hassanien, I. Sharma, K.A. Aly, Linear and nonlinear optical studies of thermally evaporated chalcogenide a-Pb-Se-Ge thin films. Physica B **613**, 412985 (2021)

2. A.S. Hassanien, H.R. Alamri, I. El Radaf, Impact of film thickness on optical properties and optoelectrical parameters of novel CuGaGeSe4 thin films synthesized by electron beam deposition. Opt. Quant. Electron. **52**(7), 1–18 (2020)

3. I. Sharma, A.S. Hassanien, Effect of Ge-addition on physical and optical properties of chalcogenide Pb10Se90-xGex bulk glasses and thin films. J. Non-Cryst. Solids **548**, 120326 (2020)

4. A.S. Hassanien, Intensive linear and nonlinear optical studies of thermally evaporated amorphous thin Cu-Ge-Se-Te films. J. Non-Cryst. Solids **586**, 121563 (2022)

5. M. Abutalib, A. Rajeh, Influence of Fe3O4 nanoparticles on the optical, magnetic and electrical properties of PMMA/PEO composites: combined FT-IR/DFT for electrochemical applications. J. Organomet. Chem. **920**, 121348 (2020)

6. L.K. Batte et al., Impact response in polymer composites from embedded optical fibers. J. Compos. Mater. **52**(25), 3415–3427 (2018)

7. H. Rezghi Maleki et al., Experimental study on drilling of jute fiber reinforced polymer composites. J. Compos. Mater. **53**(3), 283–295 (2019)

8. K. Hamdi et al., Improvement of the electrical conductivity of carbon fiber reinforced polymer by incorporation of nano-fillers and the resulting thermal and mechanical behavior. J. Compos. Mater. **52**(11), 1495–1503 (2018)

9. N. Shaari, S.K. Kamarudin, Z. Zakaria, Potential of sodium alginate/titanium oxide biomembrane nanocomposite in DMFC application. Int. J. Energy Res. **43**(14), 8057–8069 (2019)

10. M.R. Atta et al., Enhancing the structural, thermal, and dielectric properties of the polymer nanocomposites based on polymer blend and barium titanate nanoparticles for application in energy storage. Int. J. Energy Res. **46**(6), 8020–8029 (2022)

11. H.M. Alghamdi, A. Rajeh, Synthesis of carbon nanotubes/titanium dioxide and study of its effect on the optical, dielectric, and mechanical properties of polyvinyl alcohol/sodium alginate for energy storage devices. Int. J. Energy Res (2021). https://doi.org/10.1002/er.7578

12. Q.A. Alsulami, L.M. Alharbi, S.M. Keshk, Synthesis of a graphene oxide/ZnFe2O4/polyaniline nanocomposite and its structural and electrochemical characterization for supercapacitor application. Int. J. Energy Res. **46**(3), 2438–2445 (2022)

13. H. Ragab, A. Rajeh, Structural, thermal, optical and conductive properties of PAM/PVA polymer composite doped with Ag nanoparticles for electrochemical application. J. Mater. Sci.: Mater. Electron. **31**(19), 16780–16792 (2020)

14. M. Atta et al., Enhanced optical, morphological, dielectric, and conductivity properties of gold nanoparticles doped with PVA/CMC blend as an application in organoelectronic devices. J. Mater. Sci.: Mater. Electron. **32**(8), 10443–10457 (2021)

15. Z. Zakaria, S.K. Kamarudin, A review of quaternized polyvinyl alcohol as an alternative polymeric membrane in DMFCs and DEFCs. Int. J. Energy Res. **44**(8), 6223–6239 (2020)

16. Y. Altin, A. Celik Bedeloglu, Polyacrylonitrile/polyvinyl alcohol-based porous carbon nanofiber electrodes for supercapacitor applications. Int J Energy Res **45**(11), 16497–16510 (2021)

17. M.M. Abutalib, A. Rajeh, Boosting optical and electrical characteristics of polyvinyl alcohol/carboxymethyl cellulose nanocomposites by GNPs/MWCNTs fillers as an application in energy storage devices. Int. J. Energy Res. **46**(5), 6216–6224 (2022)

18. A. Hezma, A. Rajeh, M.A. Mannaa, An insight into the effect of zinc oxide nanoparticles on the structural, thermal, mechanical properties and antimicrobial activity of Cs/PVA composite. Colloids Surf., A **581**, 123821 (2019)

19. Q.A. Alsulami, A. Rajeh, Synthesis of the SWCNTs/TiO2 nanostructure and its effect study on the thermal, optical, and

conductivity properties of the CMC/PEO blend. Results in Physics **28**, 104675 (2021)

20. W. Zhou et al., Elastic deformation of multiwalled carbon nanotubes in electrospun MWCNTs–PEO and MWCNTs–PVA nanofibers. Polymer **46**(26), 12689–12695 (2005)

21. I. Elashmawi et al., Modification and development of electrical and magnetic properties of PVA/PEO incorporated with MnCl2. Physica B **434**, 57–63 (2014)

22. R.M. Putri et al., Preliminary study of electrochemical properties of polyethylene oxide (PEO) and polyvinyl alcohol (PVA) composites as material for solid polymer electrolyte. Materials Today: Proceedings **44**, 3375–3377 (2021)

23. L. Teo et al., Effect of lithium iodide on the performance of dye sensitized solar cells (DSSC) using poly (ethylene oxide)(PEO)/poly (vinyl alcohol)(PVA) based gel polymer electrolytes. Opt. Mater. **85**, 531–537 (2018)

24. M. Farea et al., Effect of cesium bromide on the structural, optical, thermal and electrical properties of polyvinyl alcohol and polyethylene oxide. J. Market. Res. **9**(2), 1530–1538 (2020)

25. A. Abdelghany et al., Structural and thermal stabilization correlation of PEO/PVA-AgCl polymer composites. Middle East J Appl Sci **5**(5), 1–6 (2015)

26. P. Dhatarwal, R. Sengwa, Structural, dielectric dispersion and relaxation, and optical properties of multiphase semicrystalline PEO/PMMA/ZnO nanocomposites. Compos. Interfaces **28**(8), 827–842 (2021)

27. P. Dhatarwal, S. Choudhary, R. Sengwa, Significantly enhanced dielectric properties and chain segmental dynamics of PEO/SnO2 nanocomposites. Polym. Bull. **78**(5), 2357–2373 (2021)

28. C. Lin et al., Influence of TiO2 nano-particles on the transport properties of composite polymer electrolyte for lithium-ion batteries. J. Power Sources **146**(1–2), 397–401 (2005)

29. J. Hu et al., Poly (ethylene oxide)-based composite polymer electrolytes embedding with ionic bond modified nanoparticles for all-solid-state lithium-ion battery. J. Membr. Sci. **575**, 200–208 (2019)

30. A. Arya, A. Sharma, Insights into the use of polyethylene oxide in energy storage/conversion devices: a critical review. J. Phys. D Appl. Phys. **50**(44), 443002 (2017)

31. K. Sundaramahalingam et al., Electrical properties of lithium bromide poly ethylene oxide/poly vinyl pyrrolidone polymer blend elctrolyte. Physica B **553**, 120–126 (2019)

32. P. Dhatarwal, R. Sengwa, Investigation on the optical properties of (PVP/PVA)/Al2O3 nanocomposite films for green disposable optoelectronics. Physica B **613**, 412989 (2021)

33. M. Brza et al., Green coordination chemistry as a novel approach to fabricate polymer: Cd (II)-complex composites: Structural and optical properties. Opt. Mater. **116**, 111062 (2021)

34. M. Abutalib, A. Rajeh, Influence of ZnO/Ag nanoparticles doping on the structural, thermal, optical and electrical properties of PAM/PEO composite. Physica B **578**, 411796 (2020)

35. M. Abutalib, A. Rajeh, Structural, thermal, optical and conductivity studies of Co/ZnO nanoparticles doped CMC polymer for solid state battery applications. Polym. Testing **91**, 106803 (2020)

36. R. Hafez, S. El-Khiyami, Effect of copper (II) nitrate 3H2O on the crystalline, optical and electrical properties of poly (vinyl alcohol) films. J. Polym. Res. **27**(2), 1–12 (2020)

37. H.M. Alghamdi, M.M. Abutalib, M.A. Mannaa, O. Nur, E.M. Abdelrazek, A. Rajeh, Modification and development of high bioactivities and environmentally safe polymer nanocomposites doped by Ni/ZnO nanohybrid for food packaging applications. J. Market. Res. **19**, 3421–3432 (2022)

38. A. Badawi, Bandgap tuning of polyvinyl alcohol capped alloyed Sn1-xCuxS nanostructures for optoelectronic applications. J. Cryst. Growth **563**, 126091 (2021)

39. M.A. Morsi, E.M. Abdelrazek, R.M. Ramadan, I.S. Elashmawi, A. Rajeh, Structural, optical, mechanical, and dielectric properties studies of carboxymethyl cellulose/polyacrylamide/lithium titanate nanocomposites films as an application in energy storage devices. Polym. Testing **114**, 107705 (2022)

40. S.F. Bdewi et al., Synthesis, structural and optical characterization of MgO nanocrystalline embedded in PVA matrix. J. Inorg. Organomet. Polym Mater. **26**(2), 326–334 (2016)

41. S. Banerjee, A. Kumar, Swift heavy ion irradiation induced modifications in the optical band gap and Urbach's tail in polyaniline nanofibers. Nucl. Instrum. Methods Phys. Res., Sect. B **269**(23), 2798–2806 (2011)

42. H.M. Ragab, N. Algethami, N.Y. Elamin, G.M. Asnag, A. Rajeh, H.S. Alzahrani, An insight into the influence of Ag/Se nanoparticles on the structural, optical, and electrical properties of Cs/PAM nanocomposites films as application in electrochemical devices. J. Mol. Struct. **1267**, 133619 (2022)

43. H.M. Alghamdi, A. Rajeh, Synthesis of CoFe2O4/MWCNTs nanohybrid and its effect on the optical, thermal, and conductivity of PVA/CMC composite as an application in electrochemical devices. J. Inorg. Organomet. Polym Mater. **32**(5), 1935–1949 (2022)

44. N.R. Kumar, V. Crasta, B. Praveen, Dielectric and electric conductivity studies of PVA (Mowiol 10–98) doped with

MWCNTs and WO3 nanocomposites films. Mater Res Express **3**(5), 055012 (2016)

45. K. Rajesh et al., Structural, optical, mechanical and dielectric properties of titanium dioxide doped PVA/PVP nanocomposite. J. Polym. Res. **26**(4), 1–10 (2019)

46. G. Shanmugam, V. Krishnakumar, Effects of anhydrous AlCl3 dopant on the structural, optical and electrical properties of PVA–PVP polymer composite films. Indian J. Phys. **92**(5), 605–613 (2018)